

# Synthesis of Iron-Doped Titanium Oxide Nanoadsorbent and Its Adsorption Characteristics for Fluoride in Drinking Water

Lin Chen, Shuai He, Bo-Yang He, Ting-Jie Wang,\* Chao-Li Su, Chang Zhang, and Yong Jin

Department of Chemical Engineering, Tsinghua University, Beijing 100084, China

**ABSTRACT:** A novel iron-doped titanium oxide adsorbent was synthesized by precipitation from a solution of  $\text{Ti}(\text{SO}_4)_2$  and  $\text{FeSO}_4$  and used for fluoride removal from drinking water. The effects of the final pH of the precipitation solution on the adsorbent structure were investigated, and optimized conditions for the synthesis were obtained. The iron doped into the titanium oxide increased the amount of active hydroxyl groups on the adsorbent surface, which increased the fluoride adsorption capacity. The optimized adsorbent had an adsorption capacity of 53.22 mg/g, obtained by fitting adsorption data to the Langmuir isotherm. The adsorption of fluoride followed second-order kinetics. The initial pH of the fluoride solution had little effect on the adsorption capacity. A thermodynamics analysis showed that the adsorption of fluoride ions onto the adsorbent was spontaneous. The adsorbent was easily regenerated with an alkali solution.

## 1. INTRODUCTION

Although the fluoride present in drinking water is essential for human health, excessive intake of fluoride causes dental and skeletal fluorosis.<sup>1</sup> This makes it necessary to treat fluoride-contaminated water to reduce the fluoride concentration to a permissible limit, which is 1.5 mg/L in WHO guidelines. Adsorption is the most efficient technology for fluoride removal from drinking water.<sup>2</sup> Therefore, it is important to synthesize an efficient and economical adsorbent for fluoride removal.

Titanium-derived adsorbents are good selective adsorbents of fluoride ions and especially arsenic compounds.<sup>3</sup> Although  $\text{TiO}_2$  exhibits a low capacity for fluoride ion exchange, titanium tetrahydroxide  $[\text{Ti}(\text{OH})_4]$  prepared by the titration of ammonia into a  $\text{TiOSO}_4$  solution can exchange fluoride ion with the high saturation capacity of 1.6 mmol/g (30.4 mg/g).<sup>3,4</sup> In order to increase the capacity for fluoride ion exchange, mesoporous titanium oxohydroxide  $[\text{TiO}_x(\text{OH})_y]$  was prepared by sol-gel hydrolysis using titanium isopropoxide at 40 °C. Zirconia *n*-propoxide (Zr:Ti = 1:9) and tetraethyl orthosilicate (Si:Ti = 1:9) were introduced into the mesoporous titanium oxohydroxide to enhance fluoride ion exchange. The adsorption capacity of mesoporous  $\text{TiO}_x(\text{OH})_y$  was slightly higher than that of  $\text{Ti}(\text{OH})_4$ .<sup>5</sup>

Li et al.<sup>6</sup> prepared Ti-Ce and Ti-La hybrid adsorbents by the hydrolysis-precipitation method at 80 °C and showed that the adsorption isotherms obeyed the Langmuir model. Their saturation adsorption capacities for fluoride were 30.6 and 46.6 mg/g on the Ti-Ce and Ti-La adsorbents, respectively. In addition, nanocrystalline titanium dioxide,<sup>7</sup> an iron(III)-titanium(IV) binary mixed oxide,<sup>8</sup> and a cerium-titanium oxide<sup>9</sup> adsorbent have been developed to remove arsenates from drinking water. However, most of these titanium-derived adsorbents were prepared by high-temperature hydrolysis or by doping with expensive metal ions.

In our previous work, an iron-titanium bimetallic oxide adsorbent synthesized by coprecipitation at a titration terminative pH of 7 was developed. It had an adsorption capacity of 47.0 mg/g.<sup>10</sup> A synergistic interaction between iron and titanium was observed in the synthesis and adsorption

processes. The theory that the iron-titanium bimetallic oxide adsorbent adsorbed fluoride ions by forming Fe-O-Ti-F bonds was confirmed. However, the need for a special treatment of ethanol washing and microwave drying in the synthesis limited its scaleup. The present work is aimed at increasing the fluoride adsorption capacity of titanium oxide by doping with iron ions using a simple treatment that can be easily used for industrial production. The synthesis of the iron-doped titanium oxide adsorbent and its adsorption behavior were investigated.

## 2. EXPERIMENTAL SECTION

**2.1. Materials.**  $\text{FeSO}_4 \cdot 7\text{H}_2\text{O}$ , ammonia (Beijing Modern Eastern Fine Chemical Ltd., China), and  $\text{Ti}(\text{SO}_4)_2 \cdot 4\text{H}_2\text{O}$  (Sinopharm Chemical Reagent Co., Ltd.) were used to prepare the adsorbents. NaF, HCl, NaOH, and  $\text{HClO}_4$  were used to prepare the solution containing the fluoride ions. Hexamethylene tetramine,  $\text{KNO}_3$ , and a ferrotitanium reagent were used to prepare the buffer solution for the fluoride concentration measurement. The chemicals used were analytical reagent grade.

**2.2. Preparation of Iron-Doped into Titanium Oxide Adsorbent.**  $\text{FeSO}_4 \cdot 7\text{H}_2\text{O}$  and  $\text{Ti}(\text{SO}_4)_2 \cdot 4\text{H}_2\text{O}$  were dissolved in deionized water at 25 °C to form a solution with a total molar concentration of 0.3 M. A 12.5% ammonia solution was slowly titrated into the solution until the pH of the solution reached a set value (called the titration terminative pH). The solution was stirred during titration. After titration, the precipitate was filtrated and washed with deionized water until the pH of the water was neutral. The precipitate was then dried at 80 °C. Finally, it was ground manually into a fine powder.

**Received:** January 11, 2012

**Revised:** September 11, 2012

**Accepted:** September 13, 2012

**Published:** September 13, 2012

**2.3. Adsorbent Characterization.** A high-resolution scanning electron microscope (JSM 7401, JEOL Co., Japan) and a high-resolution transmission electron microscope (JEM-2011, JEOL Co., Japan) were used to examine the morphology and microstructure of the adsorbents. The adsorbent crystal structure was characterized by X-ray diffraction (D8-Advance, Bruker, Germany, with Cu K $\alpha$  radiation) using a range of 10–90° at a scan speed of 10°/min. The thermal behavior of the adsorbents was characterized by a differential scanning calorimeter and thermogravimetric analysis (TGA/DSC1/16600HT, Mettler-Toledo, Germany). The elemental composition was determined by an X-ray fluorescent spectrometer (Shimadzu XRF-1800, Japan). The binding energies and atomic ratios were measured by an X-ray photoelectron spectrometer (PHI Quantera SXM, ULVAC-PHI, Japan) with an Al K $\alpha$  anode excitation source. The binding energies in the X-ray photoelectron spectrometry analysis were calibrated by the C 1s binding energy at 284.8 eV. The  $\zeta$  potential of the adsorbents was measured by a  $\zeta$  potential analyzer (ZetaPALS, Brookhaven Instruments, USA).

**2.4. Adsorption Capacity Measurement.** A fluoride solution was prepared by dissolving NaF in deionized water. A 100 mL fluoride solution with an initial concentration of 50 mg/L was placed in a conical flask. The pH of the fluoride solution was adjusted to neutral by titration of HClO<sub>4</sub> and NaOH. The initial pH of the fluoride solution was neutral in the adsorption experiments, except in the case of the investigation of the effects of the initial pH of the fluoride solution on the adsorption. A high initial fluoride concentration of 50 mg/L was used to easily distinguish the differences in the adsorption capacity of the adsorbents prepared under different experimental conditions. A total of 0.1 g of iron-doped titanium oxide adsorbent was placed in the flask. The test solution was shaken on a shaker bed at 150 rpm and kept at 25 °C for 12 h during adsorption. After adsorption equilibrium, the adsorbent was separated from the solution by a filter with a 0.22  $\mu$ m cellulose membrane. The residual fluoride concentration in the solution was measured with a fluoride-selective electrode connected to an ion meter (PXS-450, Shanghai Kang-Yi Instruments Co., Ltd., China). The measurement conditions used for the adsorption are given in the captions of the tables and figures.

**2.5. Adsorption Behavior.** **2.5.1. Adsorption Kinetics.** The adsorption kinetics of the optimized iron-doped titanium oxide adsorbent was investigated. The adsorption rate constant ( $k_{ad1}$ ) was determined for first- and second-order kinetics.<sup>11</sup>

The first-order model is

$$\frac{dq}{dt} = k_{ad1}(q_e - q) \quad (1)$$

where  $q_e$  and  $q$  (mg/g) are the amounts of fluoride adsorbed per unit mass of adsorbent at equilibrium and at time  $t$ , respectively.  $k_{ad1}$  (1/h) is the adsorption rate constant for the first-order model.

The second-order model is

$$\frac{dq}{dt} = k_{ad2}(q_e - q)^2 \quad (2)$$

where  $k_{ad2}$  (g/mg·h) is the adsorption rate constant for the second-order kinetics model.

**2.5.2. Adsorption Isotherm.** The adsorption isotherm for fluoride ion amounts adsorbed on the optimized iron-doped

titanium oxide adsorbent were fitted to the Langmuir and Freundlich isotherms. The Langmuir isotherm is

$$\frac{1}{q_e} = \frac{1}{q_{max} b} \frac{1}{C_e} + \frac{1}{q_{max}} \quad (3)$$

where  $q_{max}$  is the maximum adsorption capacity that corresponds to a complete monolayer coverage (mg/g). The Langmuir constant  $b$  is determined by the affinity of the binding sites and is a measure of the energy of adsorption (L/mg). The model assumes that the binding sites on the adsorbent surface are homogeneous; that is, all of the binding sites have the same affinity for adsorption up to a single molecular layer.<sup>12</sup>

The Freundlich model is

$$Q_e = K_f C_e^{1/n} \quad (4)$$

where  $K_f$  and  $n$  are the Freundlich constants that quantify the adsorption capacity and adsorption intensity, respectively. The Freundlich model assumes multilayer adsorption on an energetically heterogeneous surface with sites that have different affinities for adsorption.<sup>13</sup>

**2.5.3. Effects of the Initial Fluoride Solution pH.** The initial pH values of the fluoride solutions ranged from 2.5 to 10 and were adjusted by adding HClO<sub>4</sub> and NaOH. The effect of the initial fluoride solution pH on the fluoride adsorption capacity was determined.

**2.5.4. Adsorption Thermodynamics.** The standard free energy change ( $\Delta G^\circ$ ), enthalpy change ( $\Delta H^\circ$ ), and entropy change ( $\Delta S^\circ$ ) were calculated from the change of the thermodynamic equilibrium constant  $K_0$ .<sup>14</sup>

$$K_0 = \frac{C_a}{C_e} \quad (5)$$

where  $C_a$  is milligrams of fluoride adsorbed per gram of adsorbent<sup>14–16</sup> and  $C_e$  is the equilibrium concentration of the solution (mg/L). The thermodynamic equilibrium constant  $K_0$  in terms of  $\Delta H^\circ$  and  $\Delta S^\circ$  as a function of the temperature is

$$-RT \ln K_0 = \Delta G^\circ = \Delta H^\circ - T \Delta S^\circ \quad (6)$$

$$\ln K_0 = -\frac{\Delta G^\circ}{RT} = \frac{\Delta S^\circ}{R} - \frac{\Delta H^\circ}{RT} \quad (7)$$

where  $R$  is the gas constant (J/mol·K),  $T$  is the temperature (K),  $\Delta G^\circ$  is the standard free energy change (kJ/mol),  $\Delta H^\circ$  is the standard enthalpy change (kJ/mol), and  $\Delta S^\circ$  is the standard entropy change (J/mol·K).

**2.5.5. Adsorbent Regeneration.** Adsorbent regeneration was investigated using an alkali solution to desorb fluoride from the adsorbent. The operation steps were as follows:

[1] Fresh adsorbent was added to give 1 g/L in the 50 mg/L fluoride solution, and when adsorption reached equilibrium, the adsorbent was filtered, dried, and used as the exhausted adsorbent.

[2] The exhausted adsorbent was soaked in a 0.1 M NaOH solution. After 12 h, the fluoride concentration in the NaOH solution was measured. The adsorbent was filtered, washed with a HCl solution and deionized water, dried, and used as the regenerated adsorbent.

[3] The regenerated adsorbent was added to give 1 g/L in the 50 mg/L fluoride solution again to evaluate the regeneration efficiency. The regeneration was conducted for five cycles.

**Table 1. Fluoride Adsorption Capacity of the Iron-Doped Titanium Oxide Adsorbents Synthesized Using Different Titration Terminative pH Values and the Composition in the Adsorbents (Initial Feed Fe/Ti Molar Ratio =1)**

	titration terminative pH						
	3	4	5	6	7	8	9
adsorption capacity, <sup>a</sup> mg/g	34.66	35.33	37.66	28.31	6.49	6.78	1.50
molar ratio of Fe/Ti	0.25	0.28	0.35	0.41	0.56	1.11	1.04

<sup>a</sup>Initial fluoride concentration = 50 mg/L, adsorbent dose = 1 g/L, and equilibrium time = 12 h.

### 3. RESULTS AND DISCUSSION

**3.1. Optimized Adsorbent.** The initial pH of the  $\text{Ti}(\text{SO}_4)_2$  and  $\text{FeSO}_4$  solution was less than 1. As ammonia was titrated into the solution, a precipitate formed and the pH of the solution increased. Exploratory experiments showed that the titration terminative pH significantly affected the adsorption capacity of the adsorbent. Therefore, iron-doped titanium oxide adsorbents were prepared using different titration terminative pH values and with different initial feed Fe/Ti molar ratios, and their adsorption capacities were measured. The highest adsorption capacity was achieved at a terminative pH of 5 and an initial feed Fe/Ti molar ratio of 1.

The adsorption capacity of the adsorbents versus titration terminative pH at an initial feed Fe/Ti molar ratio of 1 is shown in Table 1. The adsorbents synthesized under acidic conditions had a higher adsorption capacity, and the adsorbents synthesized under basic conditions had a lower adsorption capacity. The highest capacity of 37.66 mg/g was obtained at a terminative pH of 5. In contrast, the adsorption capacity of a pure titanium oxide prepared at a titration terminative pH of 5 was only 11.46 mg/g. This indicated that the iron doped in the titanium oxide played an important role in the adsorption process. The elemental components of the adsorbents were characterized by X-ray fluorescent spectrometry. The calculated Fe/Ti molar ratios are listed in Table 1. With increasing titration terminative pH, the Fe/Ti molar ratio in the adsorbents increased from 0.25 to 1.11. When the solution pH was lower than 5 after titration, the precipitate in the solution was still milky in color, which then became coffee and got darker as the pH increased. This indicated that titanium precipitated faster and earlier because the color of titanium oxide is white and that of iron oxide is dark. This indicated that titanium precipitated faster and earlier than iron with increasing pH in the titration. In the optimized adsorbent, the Fe/Ti molar ratio was only 0.35, although the initial feed molar ratio was 1.

The transmission electron microscopy (TEM) and scanning electron microscopy (SEM) images of the optimized iron-doped titanium oxide adsorbent are shown in Figure 1. This iron-doped titanium oxide was composed of nanospheres with diameters of 3–5 nm. This nanoadsorbent powder cannot be used directly as a packed bed because it would have a low hydraulic conductivity and high pressure drop. It needs to be granulated into 1–2 or 2–3 mm granules with sufficient strength for use in a packed bed.<sup>17,18</sup>

**3.2. Characteristics of the Adsorbent Structure.** The X-ray diffraction (XRD) spectra of the iron-doped titanium oxide adsorbents obtained at different titration terminative pH values are shown in Figure 2. For comparison, titanium oxide obtained with a terminative pH of 5 and iron oxide obtained with a terminative pH of 8 are also shown. Titanium oxide had an amorphous  $\text{Ti}(\text{OH})_4$  structure, and iron oxide gave the characteristic peaks of crystalline  $\text{FeOOH}$ . However, iron-

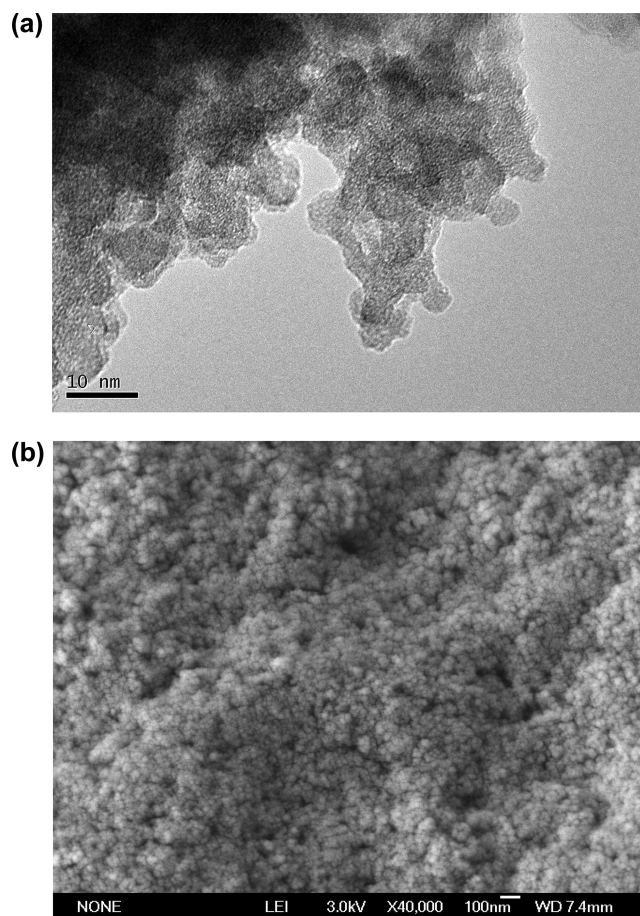


**Figure 1.** (a) TEM (a) and SEM (b) images of the optimized iron-doped titanium oxide adsorbent.

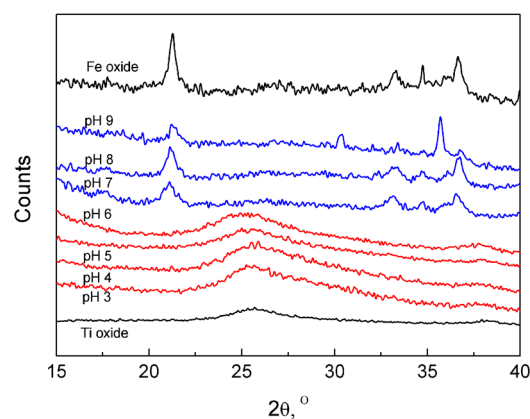


**Figure 2.** XRD spectra of the iron-doped titanium oxide adsorbents obtained with different titration terminative pH values (initial feed Fe/Ti molar ratio = 1) and those of the pure titanium oxide and iron oxide.

doped titanium oxide prepared with titration terminative pH values of 3–6 gave almost no peaks in the XRD spectra, suggesting that the formation of the crystalline phase of FeOOH was inhibited in the precipitation process. However, with titration terminative pH values of 7–9, crystalline FeOOH was gradually detected in the XRD spectra. Compared to the pure titanium oxide prepared at a titration terminative pH of 5, iron-doped titanium oxide had a higher capacity.  $\text{Ti}(\text{OH})_4$  prepared by titration of ammonia into a  $\text{TiOSO}_4$  solution reported in the literature<sup>3,4</sup> also had a lower capacity than the optimized adsorbent in this work. Together with the capacity data in Table 1, it was inferred that the amorphous  $\text{Ti}(\text{OH})_4$  structure doped with iron contributed to the higher capacity for fluoride adsorption.

Figure 3 shows the thermal weight loss characterization of the iron-doped titanium oxide adsorbents obtained with

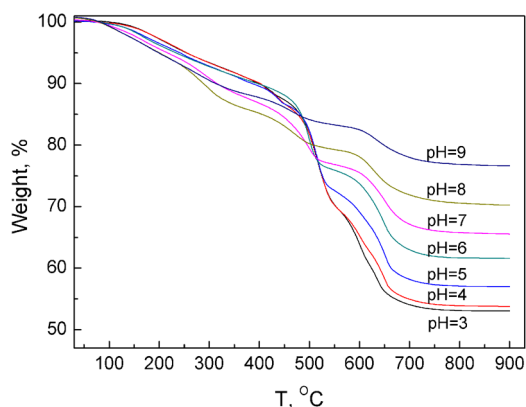


**Figure 3.** TGA curves of the iron-doped titanium oxide adsorbents obtained with different titration terminative pH values (initial feed Fe/Ti molar ratio = 1).

different terminative pH values. The weight loss of the adsorbents from 300 to 900 °C decreased as the titration terminative pH increased. In this range, bound water on the adsorbent and hydroxyl groups on the adsorbent surface were removed as the temperature increased. A higher weight loss by the adsorbent indicated a larger amount of hydroxyl groups on the adsorbent surface, which provided more active sites for fluoride adsorption.

To further analyze the characteristics of fluoride adsorption on the iron-doped titanium oxide adsorbent, the chemical change of the adsorbent surface before and after adsorption was examined by X-ray photoelectron spectrometry (XPS). Figure 4 shows the XPS spectra for the O 1s peaks of the iron-doped titanium oxide adsorbents prepared at terminative pH values of 5, 7, and 9 before and after fluoride adsorption, as well as that of the titanium oxide prepared at a terminative pH of 5. The O 1s spectrum comprised a 530.0 eV peak assigned to  $\text{O}^{2-}$  (bonded to metal) and a 531.5 eV peak assigned to  $\text{OH}^-$  (hydroxyl) groups on the surface;<sup>19</sup> that is, a larger higher binding energy O 1s peak indicated a higher density of  $\text{OH}^-$  groups on the adsorbent surface. Figure 4 showed that all iron-doped titanium oxide had a larger higher binding energy O 1s peak than that of pure titanium oxide. This suggested that iron-doped titanium oxide promoted the formation of hydroxyl groups on the adsorbent surface. Furthermore, the optimized adsorbent prepared at a terminative pH of 5 had a larger higher binding energy of the O 1s peak than those of the adsorbents prepared with pH values of 7 and 9. The solution pH in the

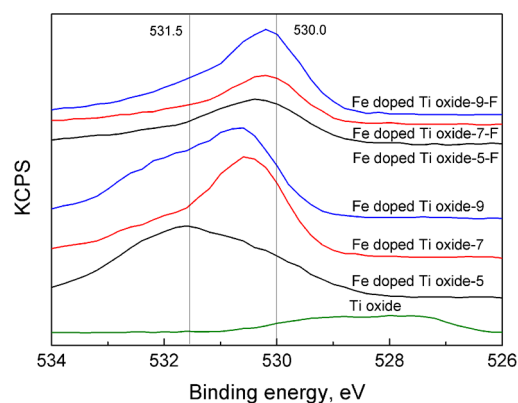


**Figure 4.** O 1s XPS spectra of the iron-doped titanium oxide adsorbent synthesized at titration terminative pH values of 5, 7, and 9 (initial feed Fe/Ti molar ratio = 1) before and after fluoride adsorption and titanium oxide synthesized at a titration terminative pH of 5.

synthesis process affected the surface and structure properties of the adsorbents. The density and properties of the hydroxyl groups on the surface of the adsorbents were determined by the surface component, structure, and active sites. The terminative pH affected the formation of active hydroxyl groups on the adsorbent surface, the amount of which determined the fluoride adsorption capacity. After fluoride adsorption, all of the O 1s peaks of the iron-doped titanium oxide adsorbents were obviously smaller, which indicated that the active  $\text{OH}^-$  groups on the adsorbent surface were consumed in the ion exchange in the fluoride adsorption.

**3.3. Adsorption Kinetics.** The amount of fluoride adsorbed versus adsorption time is plotted in Figure 5. The

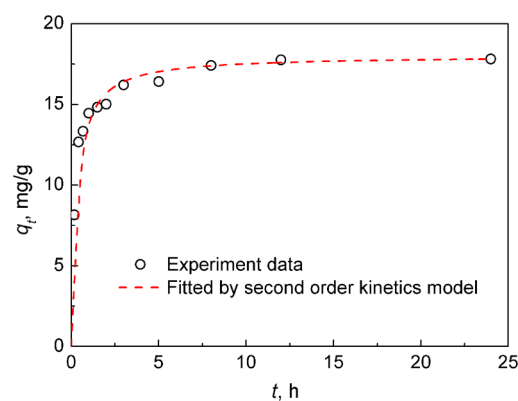


**Figure 5.** Fluoride adsorption kinetics of the optimized iron-doped titanium oxide adsorbent and the fit to the second-order kinetics model (initial fluoride concentration = 10 mg/L; adsorbent dose = 0.5 g/L).

adsorption of fluoride was rapid in the first 1 h, and then the adsorption rate slowed until equilibrium was reached at about 12 h. The calculated adsorption rate constants and other parameters are listed in Table 2. The values of  $k_{\text{ad}2}$  and  $R^2$  for the second-order kinetics model were 0.19 g/mg·h and 0.9998, respectively. The large correlation coefficient for the second-order equation showed that fluoride removal by the adsorbent followed second-order kinetics.

**3.4. Adsorption Isotherm.** The experimental data at equilibrium for fluoride ion amounts adsorbed on the optimized iron-doped titanium oxide adsorbent were fitted to

**Table 2. Fitted Parameters from First- and Second-Order Kinetics Models for the Optimized Iron-Doped Titanium Oxide Adsorbent<sup>a</sup>**

parameter	first-order kinetics model			second-order kinetics model		
	$k_{ad1}$	$q_e$	$R^2$	$k_{ad2}$	$q_e$	$R^2$
units	1/h	mg/g		g/mg·h	mg/g	
value	0.502	8.88	0.9751	0.19	18.02	0.9998

<sup>a</sup>Initial fluoride concentration = 10 mg/L and adsorbent dose = 0.5 g/L.

the Langmuir and Freundlich isotherms, which are shown in Figure 6.

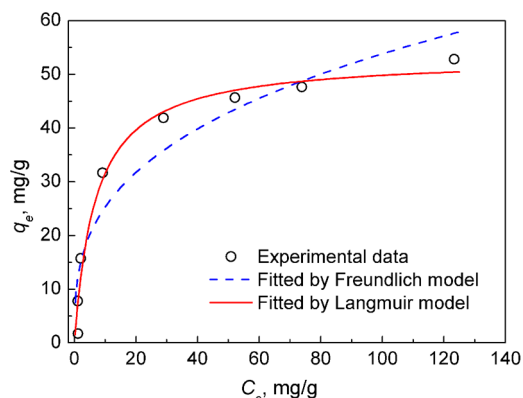


**Figure 6.** Adsorption isotherm of fluoride onto the optimized iron-doped titanium oxide adsorbent (adsorbent dose = 0.5 g/L; equilibrium time = 12 h).

In the Langmuir fit, the values of  $q_{max}$  and  $b$  were calculated from the slope and intercept of the linear plots of  $1/q_e$  versus  $1/C_e$  and were 53.22 mg/g and 0.15 L/mg, respectively. In the Freundlich fit, the values of  $K_f$  and  $n$  for the adsorbent were respectively 11.89 mg/g and 3.05. The value of  $1/n$  was less than 1, which indicated favorable adsorption.

The fitted adsorption isotherms are shown in Figure 6. The fitted values of the parameters are given in Table 3. The

**Table 3. Adsorption Isotherm Parameters of Fluoride Adsorbed onto the Optimized Iron-Doped Titanium Oxide Adsorbent<sup>a</sup>**

parameter	Freundlich isotherm model			Langmuir isotherm model		
	$K_f$	$n$	$R^2$	$q_{max}$	$b$	$R^2$
units	mg/g			mg/g	L/mg	
value	11.89	3.05	0.892	53.22	0.15	0.976

<sup>a</sup>Adsorbent dose = 0.5 g/L and equilibrium time = 12 h.

correlation coefficients of the two isotherm models showed that the experimental data were better fitted by the Langmuir isotherm. This also indicated that the adsorption on the iron-doped titanium oxide adsorbent was close to monolayer adsorption. The saturation adsorption capacity from the Langmuir isotherm was 53.22 mg/g, which was higher than that of the  $Ti(OH)_4$  adsorbent (30.4 mg/g),<sup>4</sup> Ti–Ce hybrid adsorbent (30.6 mg/g),<sup>6</sup> Ti–La hybrid adsorbent (46.6 mg/g)<sup>6</sup> and Fe–Ti bimetallic oxide adsorbent (47.0 mg/g).<sup>10</sup>

The differences between the iron-doped titanium oxide and Fe–Ti bimetallic oxide adsorbent were as follows: (1) the feed molar ratio of Fe/Ti of the former was 1, and that of the latter

was 2; (2) the titration terminative pH of the former was 5, and that of the latter was 7; (3) the former was washed with water and dried in a drying oven and can be easily scaled up, but the latter was washed with ethanol and dried in a microwave oven. The differences in the synthesis process gave the iron-doped titanium oxide adsorbent a higher adsorption capacity than the Fe–Ti bimetallic oxide. The solution pH in the synthesis process affected the surface and structure properties of the adsorbent and thus the adsorption capacity.

The content and distribution of iron-doped titanium oxide were different for these two adsorbents. The Fe/Ti molar ratio in iron-doped titanium oxide was 0.35, while the Fe/Ti molar ratio in the Fe–Ti bimetallic oxide adsorbent was 1. The particle size of iron-doped titanium oxide (3–5 nm) was smaller than that of Fe–Ti bimetallic oxide (5–7 nm). The amount of hydroxyl groups on the surface of iron-doped titanium oxide was larger than that on Fe–Ti bimetallic oxide, which benefited fluoride adsorption.

In addition,  $Ti(SO_4)_2 \cdot 4H_2O$  used as a raw material for iron-doped titanium oxide is much cheaper than titanium isopropoxide and rare-earth metal sulfate used as the raw materials in the synthesis of a titanium-derived adsorbent having a high capacity. Moreover,  $FeSO_4 \cdot 7H_2O$  is a byproduct of the  $TiO_2$  industry in the sulfate process with a large amount, has little value, and is regarded as a kind of waste. Also, the preparation method for iron-doped titanium oxide is very simple and costs little, so it would be a cost-effective adsorbent.

### 3.5. Effect of the Initial Fluoride Solution pH.

Adsorbents usually have different adsorption capacities for different values of the initial pH of the fluoride solution. The different components, structures, and active sites of the adsorbents result in different adsorption behavior for fluoride. The value of the initial fluoride solution pH affected the properties of the adsorbents. When an adsorbent is used in a packed bed, the initial pH of the inlet water is usually adjusted for a higher adsorption capacity. Figure 7 shows that the initial fluoride solution pH had little effect on the adsorption capacity of the iron-doped titanium oxide adsorbent.

The  $\zeta$  potential of the adsorbent at different solution pH values is also shown in Figure 7, which indicates that the  $pH_{zpc}$  value was about 5. Most adsorbents have a higher adsorption capacity at a lower solution pH, and the adsorption capacity decreases as the pH of the solution increases. At pH values

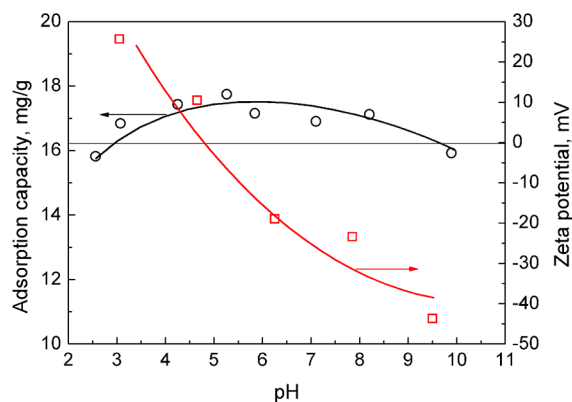
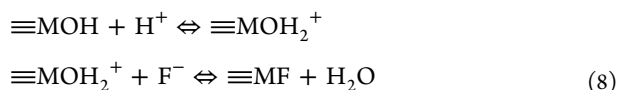


**Figure 7.** Effect of the fluoride solution pH on the fluoride amount adsorbed onto the optimized iron-doped titanium oxide adsorbent (initial fluoride concentration = 10 mg/L; adsorbent dose = 0.5 g/L; equilibrium time = 12 h).

below  $\text{pH}_{\text{zpc}}$  the surface of the adsorbent is positively charged and, hence, is accessible to fluoride ions. The following reactions occur for pH values lower than  $\text{pH}_{\text{zpc}}$ :



where  $\equiv\text{M}$  represents the metal oxide surface. At pH values above  $\text{pH}_{\text{zpc}}$  the surface of the adsorbent is negatively charged. In this case, the electrostatic attraction between the fluoride ion and the adsorbent surface decreases, and there is competitive adsorption between the hydroxyl and fluoride ions for the adsorption sites.<sup>20</sup>

According to the equation for ionization of HF,



HF forms at low solution pH, and a low solution pH promotes the formation of HF. This will lead to a reduction of the adsorption capacity for fluoride.

It is inferred that the surface potential, the HF formation at low pH, and the unique properties of the iron-doped titanium oxide adsorbent resulted in the fact that the initial solution pH had little effect on the adsorption capacity, which was observed in the experiment. A high adsorption capacity for fluoride was achieved near neutral pH. It was inferred that no pH adjustment is required in the treatment of drinking water with a natural pH around 7. The optimized iron-doped titanium oxide adsorbent showed good potential for use for the treatment of fluoride-contaminated drinking water.

**3.6. Adsorption Thermodynamics.** The values of  $\Delta H^\circ$  and  $\Delta S^\circ$  were obtained from the slope and intercept of a plot of  $\ln K_0$  against  $1/T$ . The values of  $\Delta G^\circ$ ,  $\Delta H^\circ$ , and  $\Delta S^\circ$  are given in Table 4. The negative enthalpy change indicated that fluoride

**Table 4. Adsorption Thermodynamics of the Optimized Iron-Doped Titanium Oxide Adsorbent<sup>a</sup>**

T (K)	$K_0$	$\Delta G^\circ$ (kJ/mol)	$\Delta S^\circ$ (J/mol-K)	$\Delta H^\circ$ (kJ/mol)
288	9.76	-5.46	-29.38	-13.9
298	8.00	-5.15		
308	6.70	-4.87		

<sup>a</sup>Initial fluoride concentration = 10 mg/L, adsorbent dose = 0.5 g/L, and equilibrium time = 12 h.

adsorption on iron-doped titanium oxide was exothermic. The negative entropy change during adsorption was due to the loss of the translational degree of freedom.<sup>21,22</sup> The negative free energy change at the different temperatures indicated the feasibility of the process and its spontaneous nature.

**3.7. Adsorbent Regeneration.** An alkali solution was used to regenerate the exhausted adsorbent, during which the fluoride adsorbed on the adsorbent was exchanged by hydroxide groups. The concentration of the fluoride desorbed from the adsorbent in a 0.1 M NaOH solution was measured, which is equal to the amount of fluoride adsorbed by the adsorbent. It showed that the fluoride adsorbed was totally desorbed in each cycle. The adsorption capacities of the fresh adsorbent and each regenerated adsorbent were measured and shown in Figure 8. Metal oxide adsorbents with a high density of hydroxide groups usually have a high adsorption capacity for fluoride ions. However, only active hydroxide groups adsorb fluoride ions. In the regeneration process, the fluoride ions adsorbed on the adsorbent surface were desorbed and

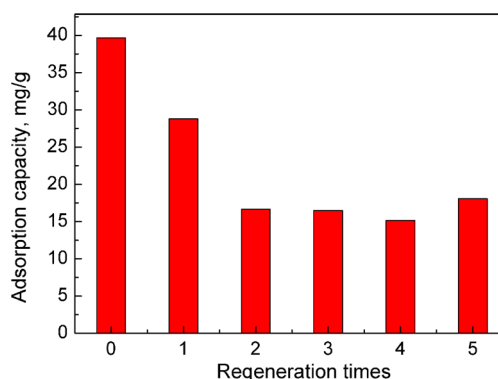


**Figure 8.** Adsorption capacities of the adsorbents after regeneration (the optimized iron-doped titanium oxide adsorbent; adsorbent dose = 1 g/L; initial fluoride concentration = 50 mg/L).

exchanged with new hydroxide groups. Some of the substituted hydroxide groups do not have activity, which caused a decrease in the regeneration efficiency. Although the adsorption capacities of the regenerated adsorbent were decreased, the adsorbent can still be applied in a continuous column where adsorption and regeneration of the adsorbent can be conducted easily and smoothly to adsorb/desorb fluoride.

#### 4. CONCLUSIONS

A cost-effective iron-doped titanium oxide adsorbent was synthesized by precipitation from  $\text{Ti}(\text{SO}_4)_2$  and  $\text{FeSO}_4$  solutions for use for fluoride removal from drinking water. The optimized adsorbent was prepared at a titration terminative pH of 5 and an initial feed Fe/Ti molar ratio of 1. The saturation adsorption capacity obtained from the Langmuir isotherm was 53.22 mg/g. The Fe/Ti molar ratio was 0.35 in the optimized adsorbent because titanium ions precipitated faster and earlier than iron ions during the titration. Iron doped into titanium oxide promoted the formation of active hydroxyl groups on the adsorbent surface, which increased the fluoride adsorption capacity. Adsorption of fluoride on the iron doped into the titanium oxide adsorbent followed second-order kinetics. The initial fluoride solution pH had little effect on the adsorption capacity. A thermodynamics analysis showed that the adsorption occurred spontaneously. The adsorbent was regenerated easily and smoothly.

#### ■ AUTHOR INFORMATION

##### Corresponding Author

\*Tel: +86-10-62788993. Fax: +86-10-62772051. E-mail: wangtj@tsinghua.edu.cn.

##### Notes

The authors declare no competing financial interest.

#### ■ ACKNOWLEDGMENTS

The authors express their appreciation of financial support of this study by the National High Technology Research and Development Program of China (863 Program, No. 2012AA062027) and the National Natural Science Foundation of China (Grants 21176134 and 20906055).

#### ■ REFERENCES

(1) Ayooob, S.; Gupta, A. K. Fluoride in drinking water: A review on the status and stress effects. *Crit. Rev. Environ. Sci. Technol.* **2006**, *36*, 433.

(2) Ayooob, S.; Gupta, A. K.; Bhat, V. T. A conceptual overview on sustainable technologies for the defluoridation of drinking water. *Crit. Rev. Environ. Sci. Technol.* **2008**, *38*, 401.

(3) Wajima, T.; Umeta, Y.; Narita, S.; Sugawara, K. Adsorption behavior of fluoride ions using a titanium hydroxide-derived adsorbent. *Desalination* **2009**, *249*, 323.

(4) Ishihara, T.; Shuto, Y.; Ueshima, S.; Ngee, H. L.; Nishiguchi, H.; Takita, Y. Titanium hydroxide as a new inorganic fluoride ion exchanger. *J. Ceram. Soc. Jpn.* **2002**, *110*, 801.

(5) Ho, L. N.; Ishihara, T.; Ueshima, S.; Nishiguchi, H.; Takita, Y. Removal of fluoride from water through ion exchange by mesoporous Ti oxohydroxide. *J. Colloid Interface Sci.* **2004**, *272*, 399.

(6) Li, Z. J.; Deng, S. B.; Zhang, X. Y.; Zhou, W.; Huang, J.; Yu, G. Removal of fluoride from water using titanium-based adsorbents. *Front. Environ. Sci. Eng. China* **2010**, *4*, 414.

(7) Pena, M.; Meng, X. G.; Korfiatis, G. P.; Jing, C. Y. Adsorption mechanism of arsenic on nanocrystalline titanium dioxide. *Environ. Sci. Technol.* **2006**, *40*, 1257.

(8) Gupta, K.; Ghosh, U. C. Arsenic removal using hydrous nanostructure iron(III)–titanium(IV) binary mixed oxide from aqueous solution. *J. Hazard. Mater.* **2009**, *161*, 884.

(9) Deng, S. B.; Li, Z. J.; Huang, J.; Yu, G. Preparation, characterization and application of a Ce–Ti oxide adsorbent for enhanced removal of arsenate from water. *J. Hazard. Mater.* **2010**, *179*, 1014.

(10) Chen, L.; He, B. Y.; He, S.; Wang, T. J.; Su, C. L.; Jin, Y. Fe–Ti oxide nano-adsorbent synthesized by co-precipitation for fluoride removal from drinking water and its adsorption mechanism. *Powder Technol.* **2012**, *227*, 3.

(11) Ho, Y. S.; McKay, G. The kinetics of sorption of divalent metal ions onto sphagnum moss flat. *Water Res.* **2000**, *34*, 735.

(12) Langmuir, I. The adsorption of gases on plane surfaces of glass mica and platinum. *J. Am. Chem. Soc.* **1918**, *40*, 1361.

(13) Zhang, T.; Li, Q. R.; Liu, Y.; Duan, Y. L.; Zhang, W. Y. Equilibrium and kinetics studies of fluoride ions adsorption on CeO<sub>2</sub>/Al<sub>2</sub>O<sub>3</sub> composites pretreated with non-thermal plasma. *Chem. Eng. J.* **2011**, *168*, 665.

(14) Niwas, R.; Gupta, U.; Khan, A. A.; Varshney, K. G. The adsorption of phosphamido on the surface of styrene supported zirconium(IV) tungstophosphate: a thermodynamic study. *Colloids Surf., A* **2000**, *164*, 115.

(15) Li, Y.; Zhang, P.; Du, Q.; Peng, X.; Liu, T.; Wang, Z.; Xia, Y.; Zhang, W.; Wang, K.; Zhu, H.; Wu, D. Adsorption of fluoride from aqueous solution by graphene. *J. Colloid Interface Sci.* **2011**, *363*, 348.

(16) Mandal, S.; Mayadevi, S. Defluoridation of water using as-synthesized Zn/Al/Cl anionic clay adsorbent: Equilibrium and regeneration studies. *J. Hazard. Mater.* **2009**, *167*, 873.

(17) Wu, H. X.; Wang, T. J.; Dou, X. M.; Zhao, B.; Chen, L.; Jin, Y. Spray coating of adsorbent with polymer latex on sand particles for fluoride removal in drinking water. *Ind. Eng. Chem. Res.* **2008**, *47*, 4697.

(18) Chen, L.; Wang, T. J.; Wu, H. X.; Jin, Y.; Zhang, Y.; Dou, X. M. Optimization of a Fe–Al–Ce nano-adsorbent granulation process that used spray coating in a fluidized bed for fluoride removal from drinking water. *Powder Technol.* **2011**, *206*, 291.

(19) Sanjines, R.; Tang, H.; Berger, H.; Gozzo, F.; Margaritondo, G.; Levy, F. Electronic structure of anatase TiO<sub>2</sub> oxide. *J. Appl. Phys.* **1994**, *75*, 2945.

(20) Wu, H. X.; Wang, T. J.; Chen, L.; Jin, Y.; Zhang, Y.; Dou, X. M. The Roles of the Surface Charge and Hydroxyl Group on a Fe–Al–Ce Adsorbent in Fluoride Adsorption. *Ind. Eng. Chem. Res.* **2009**, *48*, 4530.

(21) Gopal, V.; Elango, K. P. Equilibrium, kinetic and thermodynamic studies of adsorption of fluoride onto plaster of Paris. *J. Hazard. Mater.* **2007**, *141*, 98.

(22) Chen, S. Y.; Shen, W.; Yu, F.; Wang, H. P. Kinetic and thermodynamic studies of adsorption of Cu<sup>2+</sup> and Pb<sup>2+</sup> onto amidoximated bacterial cellulose. *Polym. Bull.* **2009**, *63*, 283.